Supporting Information

Tailoring the electric structure by constructing the heterointerface of RuO_2-NiO for overall water splitting with ultralow overpotential and extra-long lifetime over 2000 hours at 1000 mA/cm²

Gengwei Zhang,[a] Bin Wang, [a] Lu Li,[a] Sen Yang,[a] Jiamei Liu [b] and Shengchun Yang[a*]*

a School of Science, MOE Key Laboratory for Non-equilibrium Synthesis and Modulation of Condensed Matter, State Key Laboratory for Mechanical Behavior of Materials, Xi'an Jiaotong University, No. 28 West Xianning Road, Xi'an 710049, China
b Instrument Analysis Center of Xi'an Jiaotong University, Xi'an Jiaotong University, No.28, Xianning West Road, Xi'an, Shaanxi, 710049, China
E-mail: bin_wang@xjtu.edu.cn (B. Wang); ysch1209@mail.xjtu.edu.cn. (S. Yang)

EXPERIMENTAL

Materials. KOH and RuO_2 were purchased from MACKLIN Reagent Co. $RuCl_3$ was obtained from the Kunming institute of precious metals. Nickel foam, Pt/C was purchased from Alfa Aesar Chemical Reagent Co. All chemicals were used as received without further purification. Ultrapure water (18.2 MΩ cm) was used in all the experiments.

Characterizations

The structural characterization was investigated by X-ray diffraction on a Bruker-AXS D8 Advance diffractometer using Cu Kα radiation (λ = 1.5418 Å). The morphology of the as-produced samples was characterized by scanning electron microscope (FEI Quanta, FEG 250, energy spectrum: EDAX, Apollo XL-SDD). The TEM images of the products were recorded on a JEOL JEM-2100 transmission electron microscope. High-angle annular dark-field scanning transmission electron microscopy and energy-dispersive X-ray spectroscopy mapping were determined by JEOL JEM-F200. The chemical state of the samples was measured by the X-ray photoelectron spectroscopy

(Kratos, AXIS ULtrabld). The composition of the catalyst was determined by inductively coupled plasma emission spectroscopy (ICP-AES 5300). The RuO_2-NiO/NF sample was dissolved in a Teflon-lined stainless steel reactor with aqua regia at 180℃ for 8 h[1]. The concentration of the Ru and Ni dissolved in the electrolyte during the water electrolysis was determined by ICP-AES. The electrolyte of each 100 h was transferred into volumetric flask to make 100 mL, and examined by ICP-OES analysis

Model and computation detail

The calculations were carried out with the density functional theory (DFT) as implemented in the Vienna ab initio simulation package (VASP). The exchange-correlation functional was described within the generalized gradient approximation (GGA) parameterized by the Perdew-Burke-Ernzerhof (PBE). The vdW correction was considered by employing the Grimme's D3. To describe the interactions between valence electrons and the ion core. The cut-off energy for the plane-wave basis was set to 400 eV. To better describe Coulomb interaction in the localized 3d orbitals and magnetic interaction, an effective U of 5.3 eV for Ni d-states was used in this study[2, 3]. A vacuum region of 15 Å perpendicular to the surface was applied to avoid interaction between neighboring surfaces. Atoms were relaxed until the Hellmann-Feynman forces acting on them were less than 0.02 eV/Å. NiO was modeled as a (2 × 2) surface unit cell of three-layered NiO (100). RuO_2 was modeled as a (2 × 2) surface unit cell of three-layered RuO_2 (110). To simulate the RuO_2-NiO interface, an inverse model was used in which a NiO ribbon was deposited on a three-layer RuO_2 (110) slab[2]. The Brillouin zone was sampled by a (3×3×1) Gamma-centered k-mesh. The reaction barriers of water dissociation were determined by climbing-image nudged elastic band method, with six images placed between the reactant and product geometries[4]. The adsorption free energy for adsorbates (ΔG_{ads}) in HER and OER can be calculated by the following equation:

$$\Delta G_{ads} = \Delta E_{ads} + \Delta E_{ZPE} - T\Delta S \quad (1)$$

where ΔE_{ads} is the adsorption energy of adsorbates, and T is temperature. ΔE_{ZPE} and ΔS are the energy difference in zero point energy and entropy, respectively, which were obtained based on vibration analysis. The hydrogen adsorption free energy (ΔG_{H*}) is expressed as

$$\Delta G_{H*} = \Delta E_{H*} + \Delta E_{ZPE} - T\Delta S \quad (2)$$

the ΔE_{H*} can be calculated from

$$\Delta E_{H*} = E(H*) - E(*) - 1/2E_{H2} \quad (3)$$

where $E(H*)$ and $E(*)$ are the DFT energies of the given surface with and without H adsorption respectively and $E(H_2)$ is the DFT energy of a molecular H_2 in gas phase. OER activity is evaluated by the following four elementary steps[5].

$$(1)\ H_2O + * \rightarrow HO* + H^+ + e^- \quad (4)$$

$$(2)\ HO* \rightarrow O* + H^+ + e^- \quad (5)$$

$$(3)\ O* + H_2O \rightarrow HOO* + H^+ + e^- \quad (6)$$

$$(4)\ HOO* \rightarrow * + O_2 + H^+ + e^- \quad (7)$$

The adsorption energy of intermediates (O*, OH*, OOH*) on (*) substrate were determined by the following approach of Nøeskov et al[5].

$$\Delta E_{O*} = E_{OH*} - E_{(*)} - (E_{H2O} - 1/2E_{H2}) \quad (8)$$

$$\Delta E_{OH*} = E_{O*} - \Delta E_{(*)} - (E_{H2O} - E_{H2}) \quad (9)$$

$$\Delta E_{OOH*} = E_{OOH*} - \Delta E_{(*)} - (2E_{H2O} - 3/2E_{H2}) \quad (10)$$

Where $E_{(*)}$, E_{HO*}, E_{O*}, and E_{HOO*} are the total energies of the pure surface and the adsorbed surface with HO*, O*, and HOO*, respectively, E_{H2O} are the computed energies for the sole H_2O molecule. The Gibbs free energy changes for steps 4-7 can be expressed as follows:

$$\Delta G_1 = \Delta G_{OH*} - eU \quad (11)$$

$$\Delta G_2 = \Delta G_{O*} - \Delta G_{OH*} - eU \quad (12)$$

$$\Delta G_3 = \Delta G_{OOH*} - \Delta G_{O*} - eU \quad (13)$$

$$\Delta G_4 = 4.92 - \Delta G_{OOH*} - eU \quad (14)$$

Where U is the applied voltage. The theoretical overpotentials (η) for OER can be calculated by the following equations:

$$G_{OER} = max\ \{\Delta G_1, \Delta G_2, \Delta G_3, \Delta G_4\} \quad (15)$$

$$\eta = G_{OER}/e - 1.23\ \text{V} \quad (16)$$

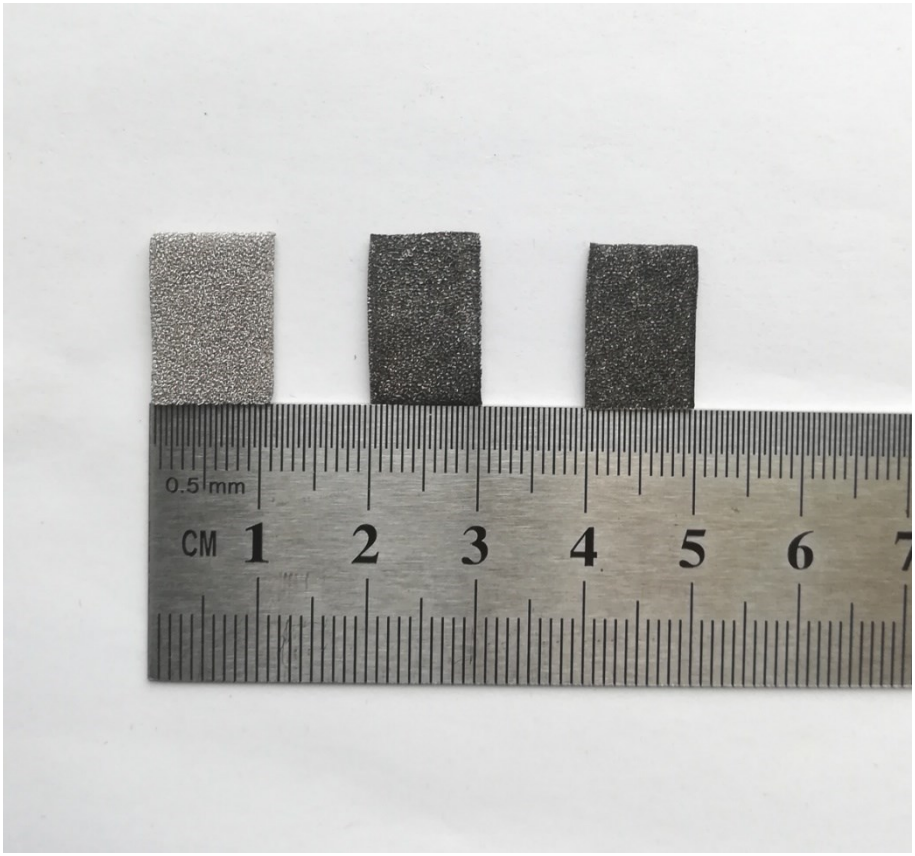

Fig. S1 Photo of bare NF, pre-RuO_2-NiO/NF and RuO_2-NiO/NF from left to right.

Fig. S2 Photo of the RuO_2-NiO/NF with an area of 200 cm^2.

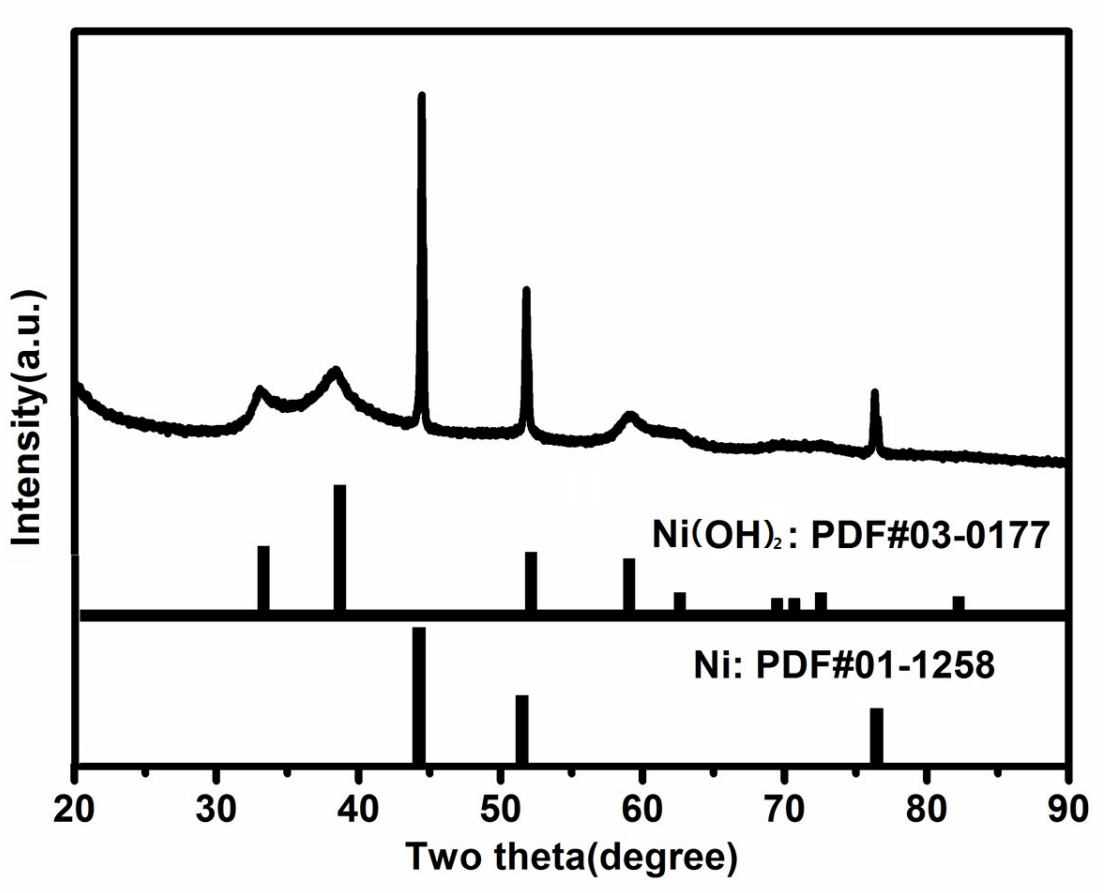

Fig. S3 XRD pattern of pre-RuO_2-NiO/NF.

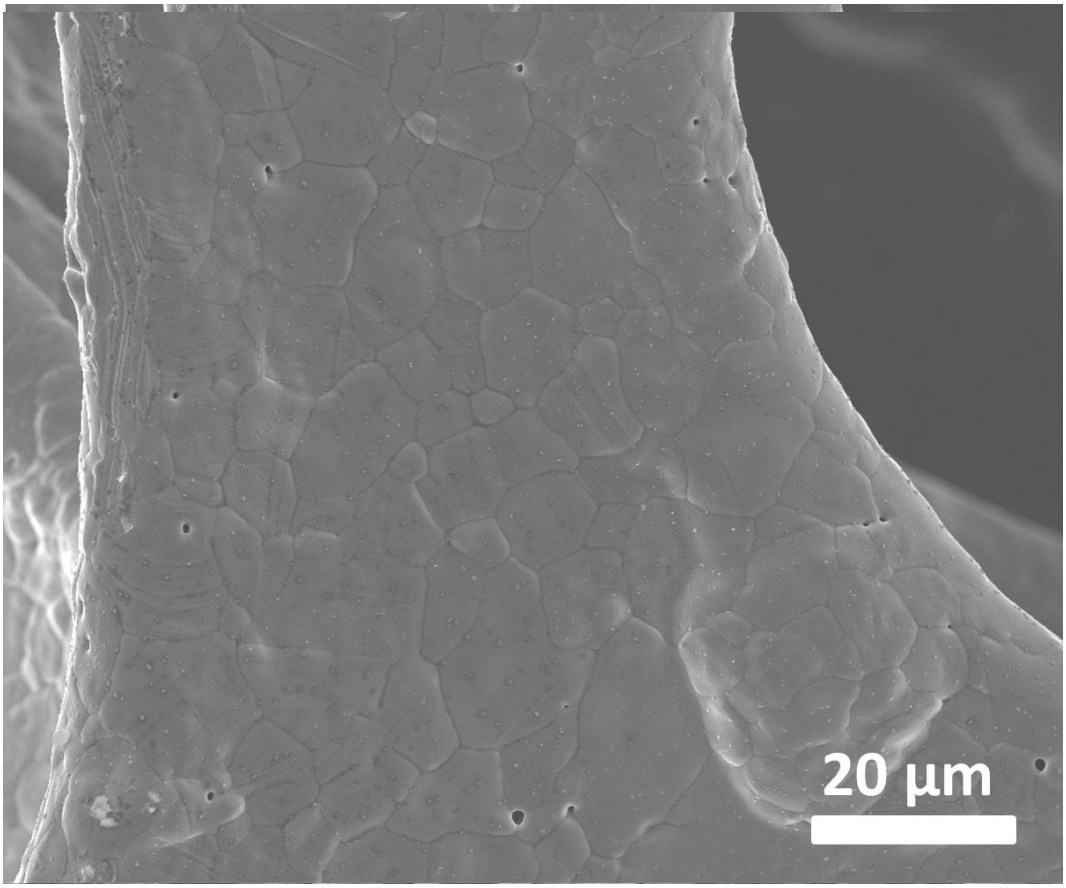

Fig. S4 SEM image of blank nickel foam.

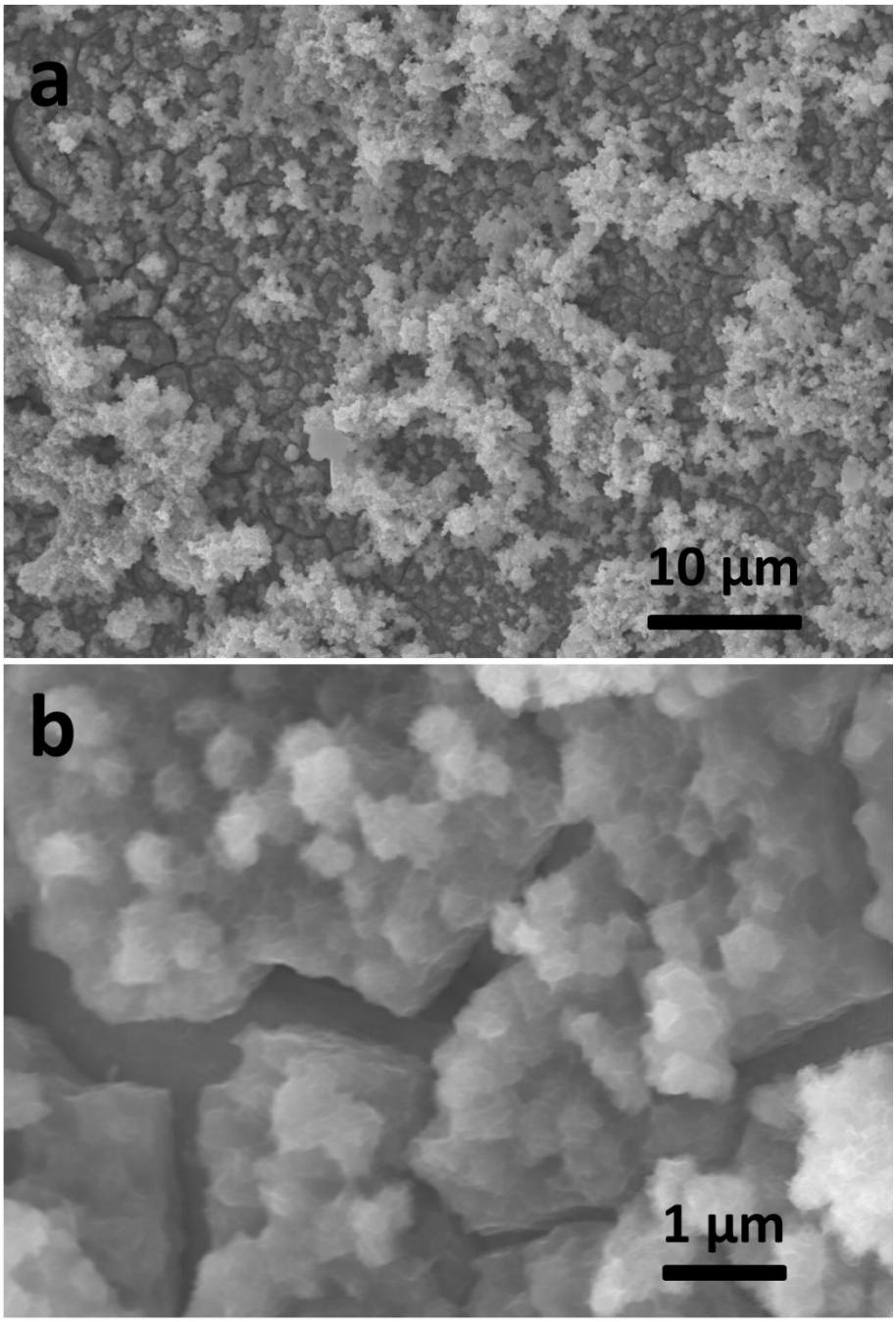

Fig. S5 Low and high magnification SEM images of pre-RuO_2-NiO/NF.

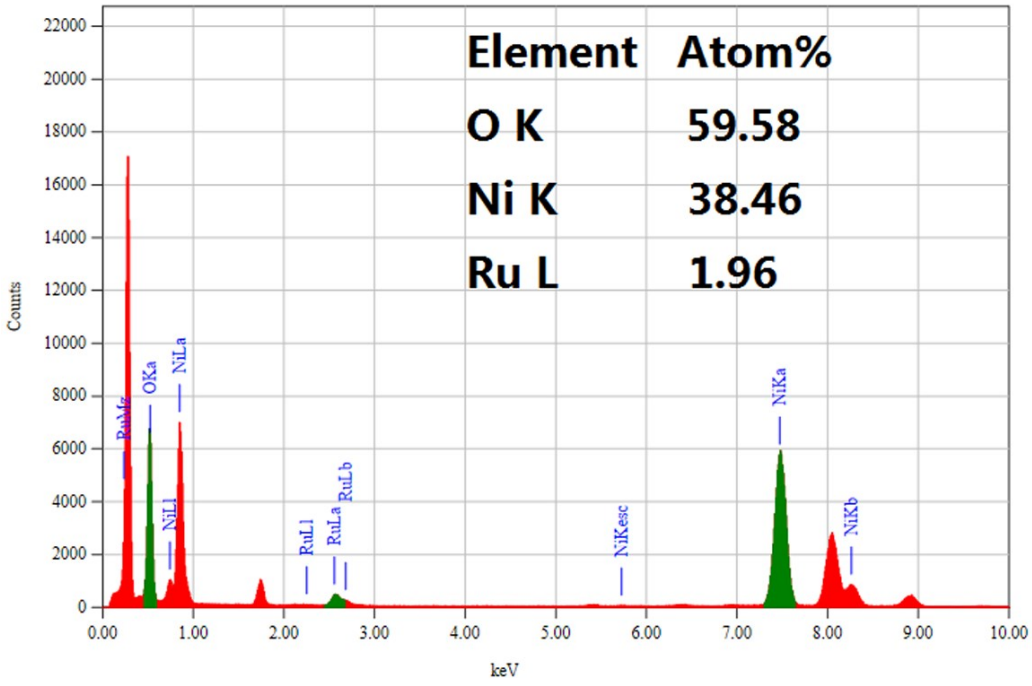

Fig. S6 The EDX spectrum of RuO_2-NiO nanoparticles.

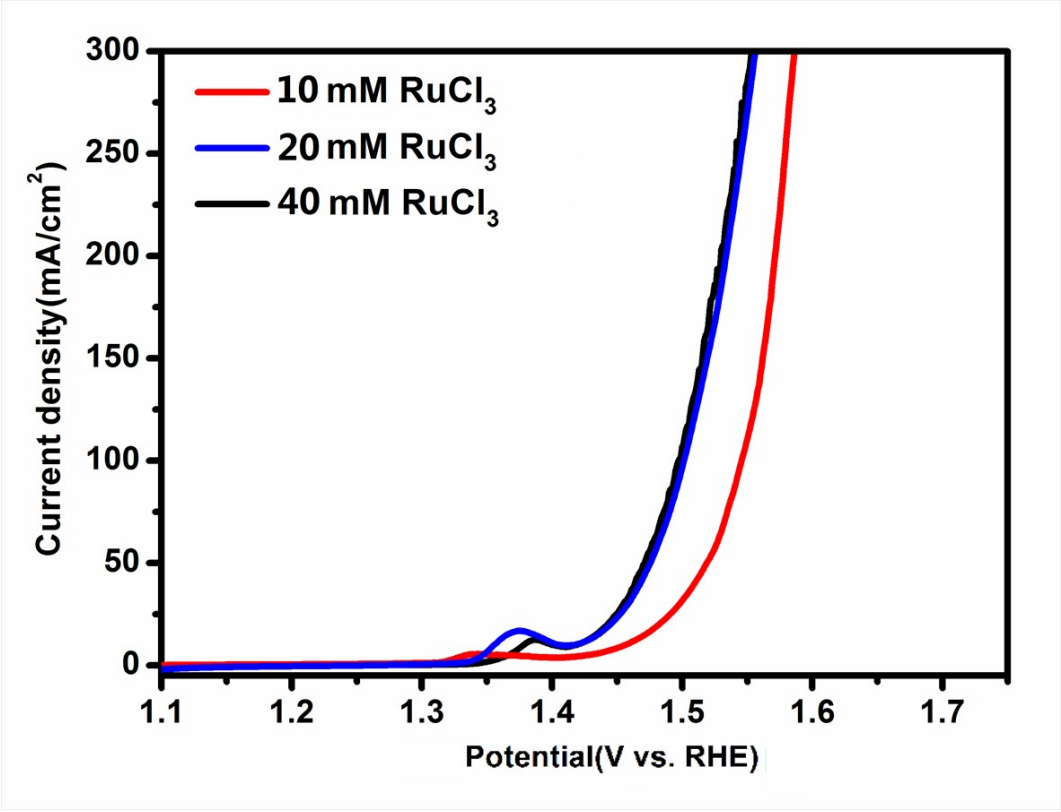

Fig. S7 The LSV curves of RuO_2-NiO/NF with different RuO_2 loading amount for OER in 1 M KOH.

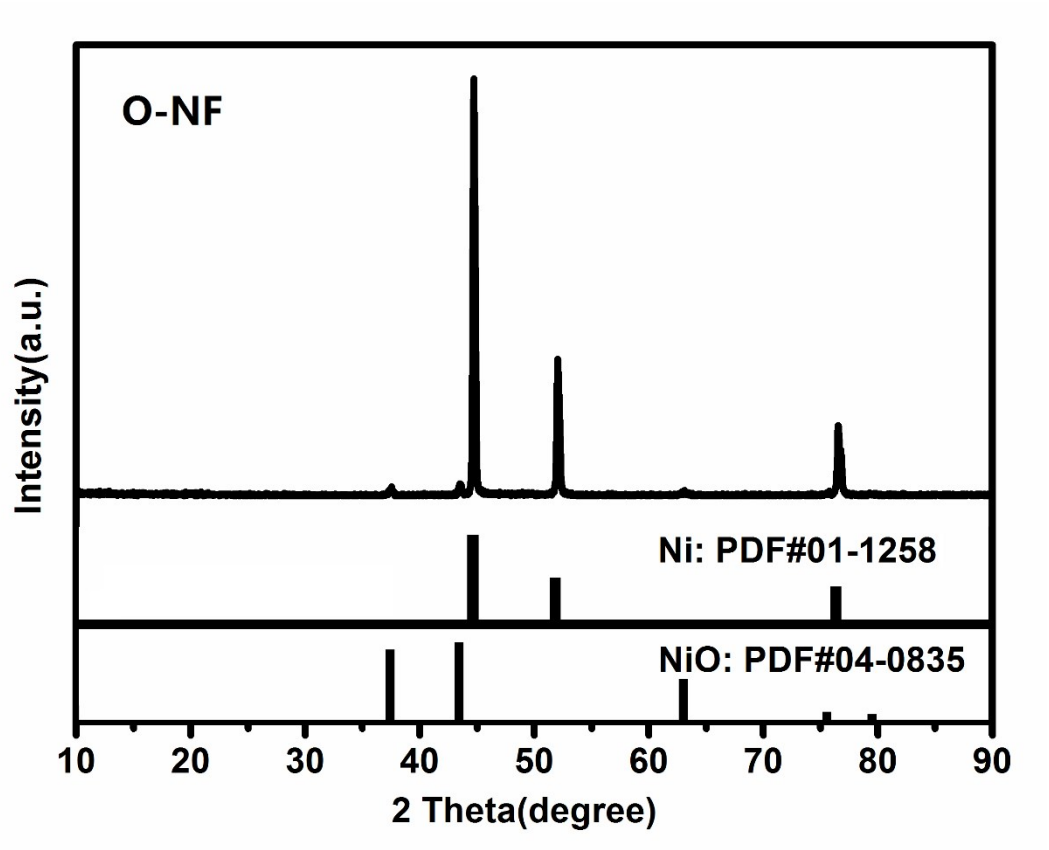

Fig. S8 XRD pattern of O-NF.

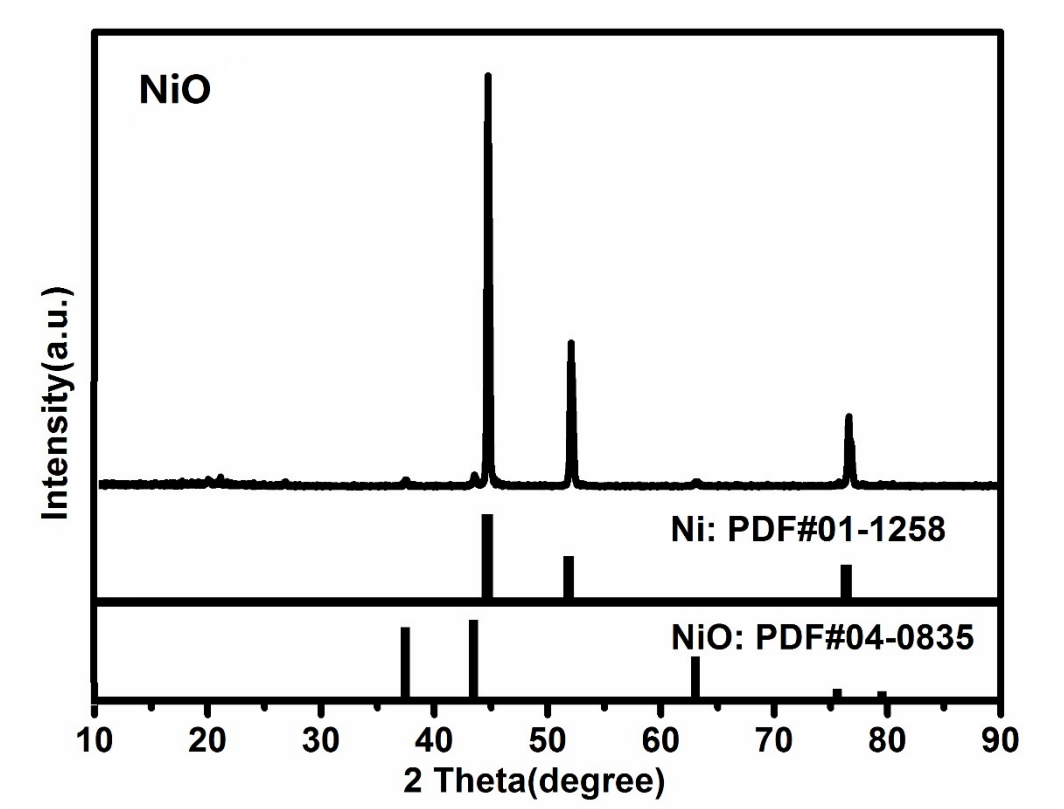

Fig. S9 XRD pattern of NiO/NF.

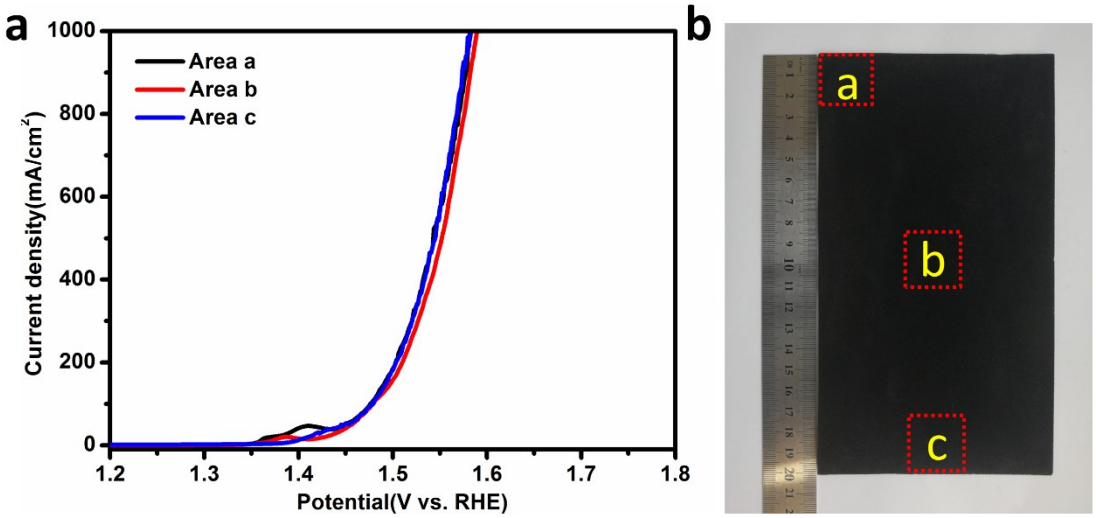

Fig. S10 The LSV curves of different part of RuO_2-NiO/NF prepared with a large area.

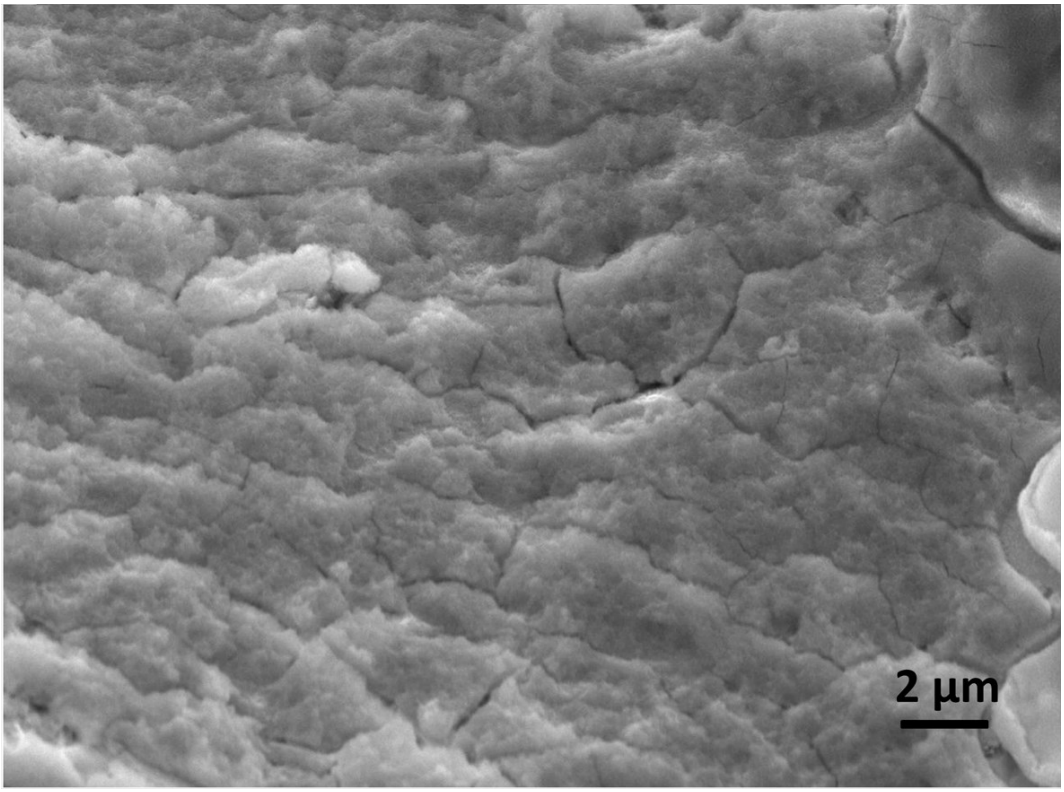

Fig. S11 The SEM image of RuO_2-NiO/NF after the OER stability test.

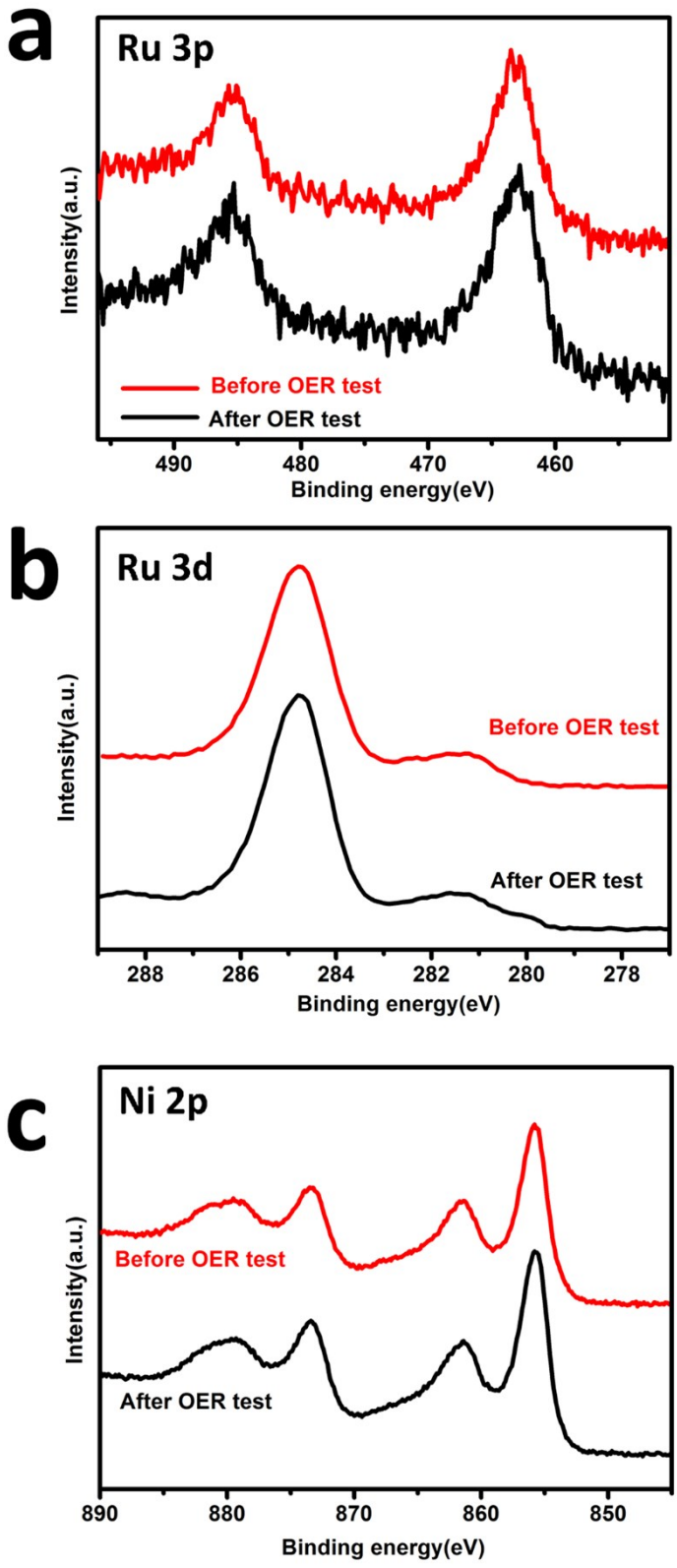

Fig. S12 High-resolution XPS spectra of (a) Ru 3p, (b) Ru 3d and (c) Ni 2p of RuO_2-NiO/NF before and after OER test, respectively.

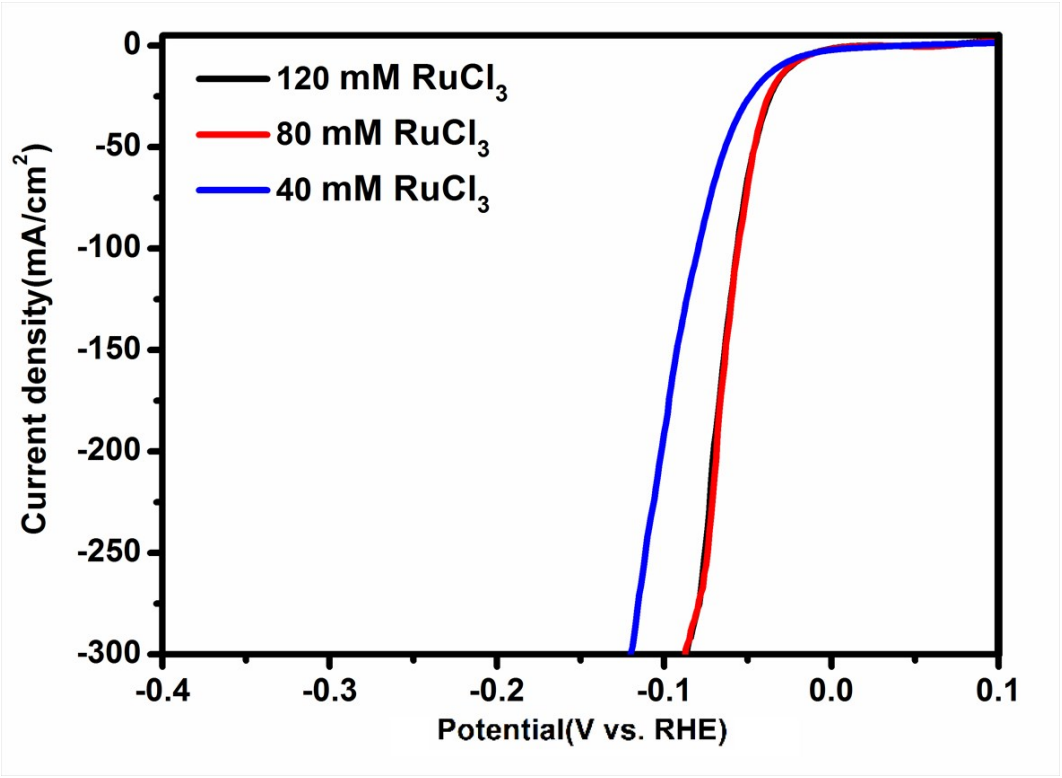

Fig. S13 The LSV curves of RuO_2-NiO/NF with different RuO_2 loading amount for HER in 1 M KOH.

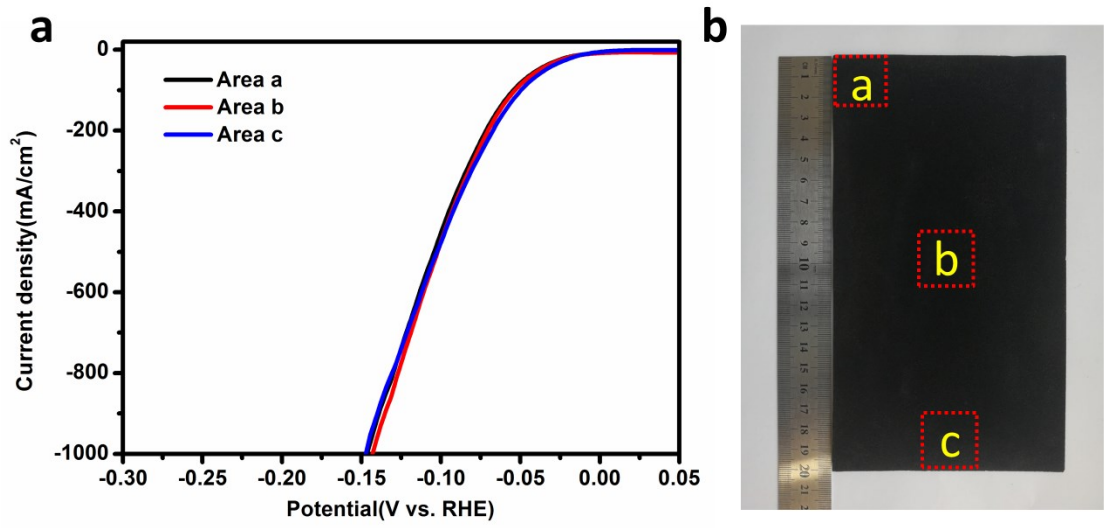

Fig. S14 The LSV curves of different part of RuO_2-NiO/NF prepared with a large area.

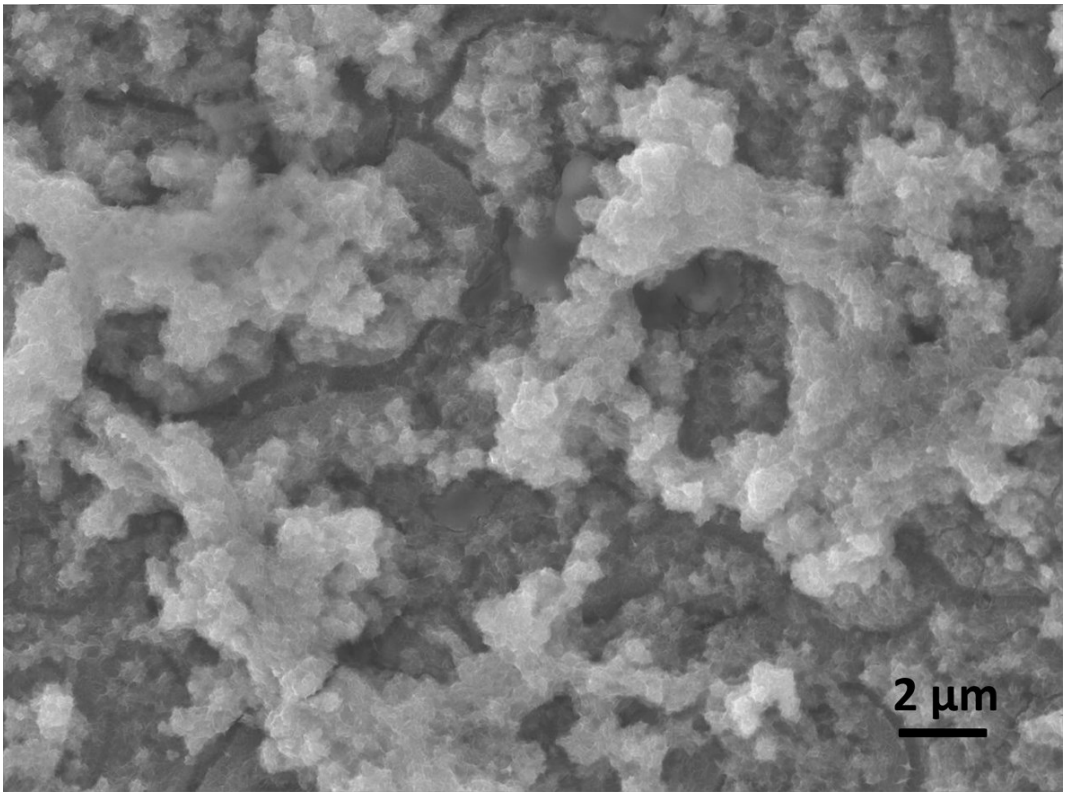

Fig. S15 The SEM image of RuO_2-NiO/NF after the HER stability test.

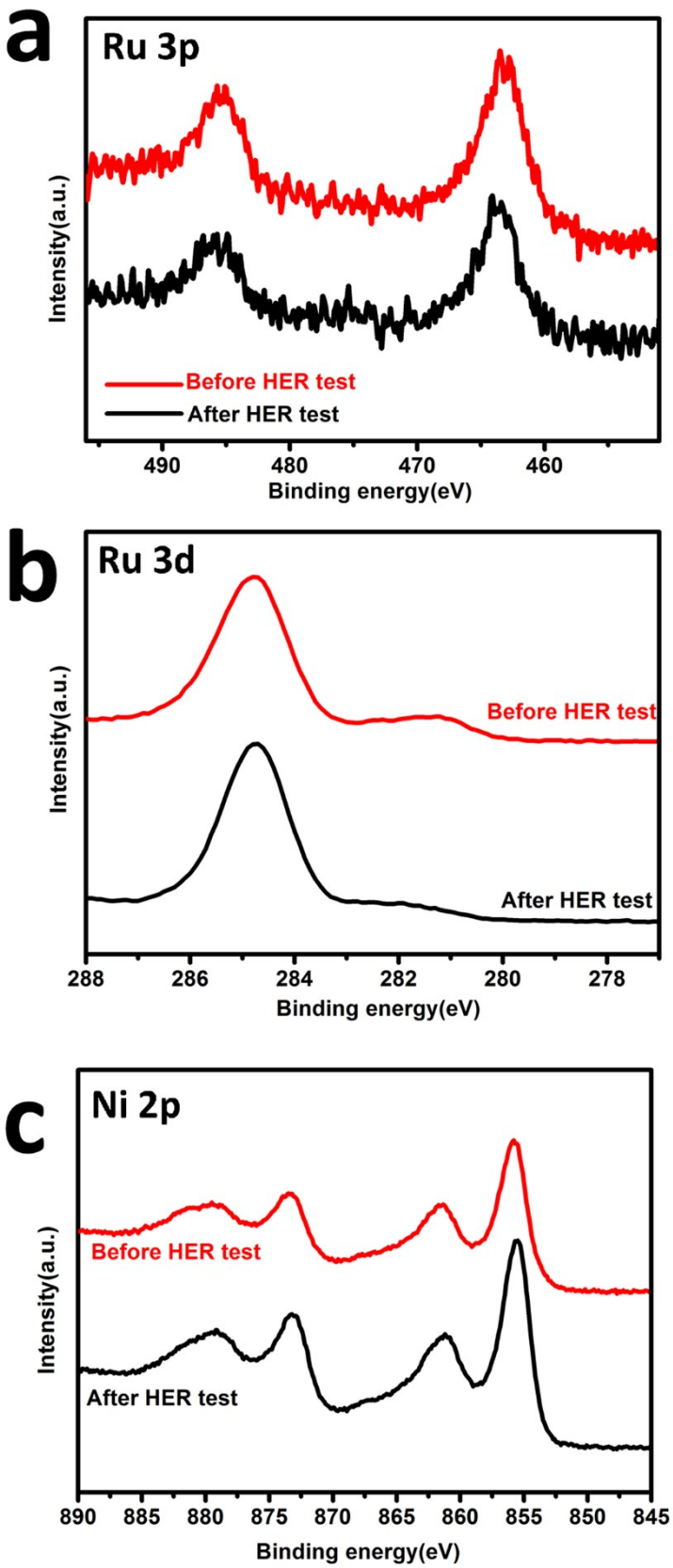

Fig. S16 The high-resolution XPS spectra of (a) Ru 3p, (b) Ru 3d and (c) Ni 2p of RuO_2-NiO/NF before and after HER test.

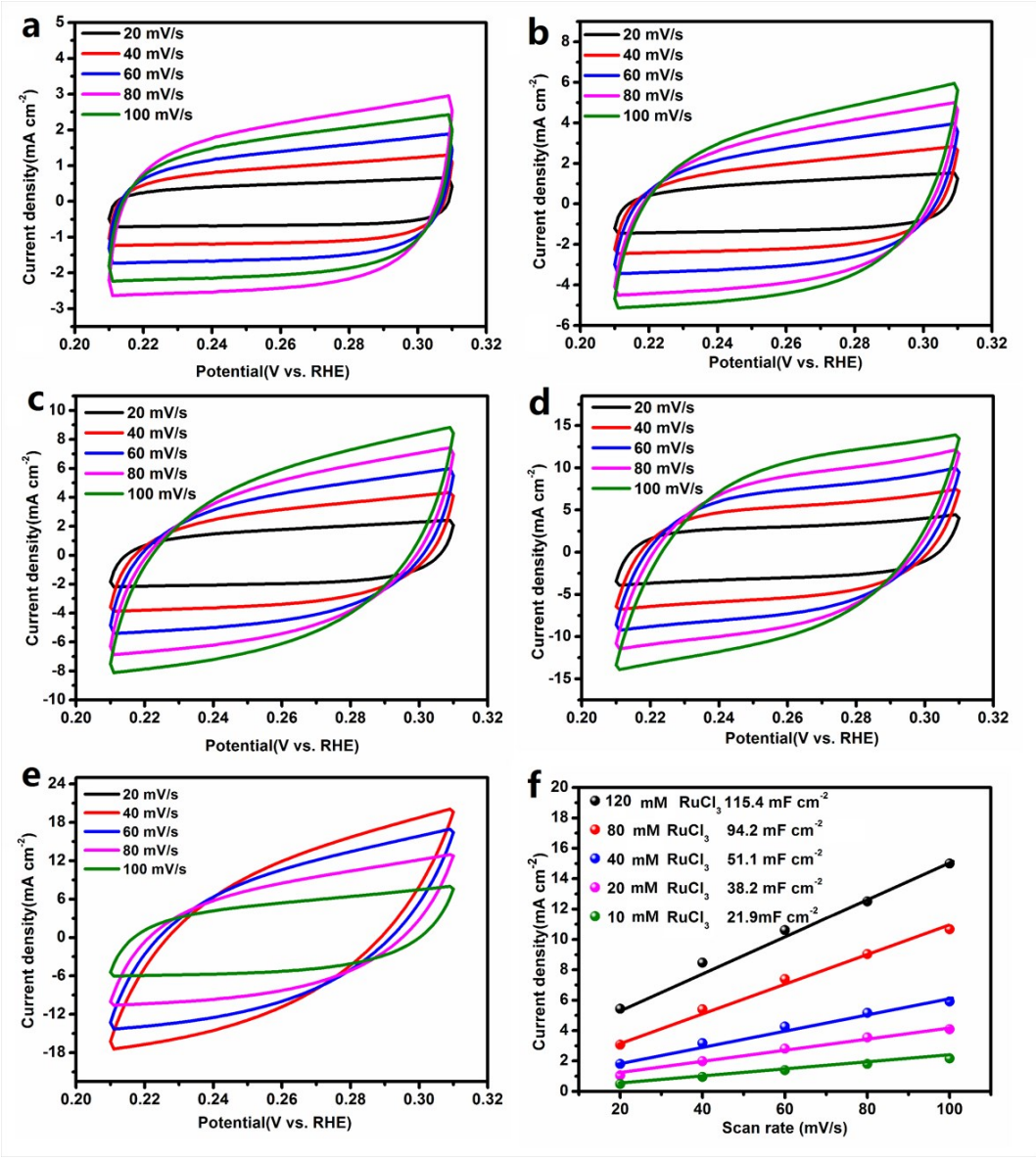

Fig. S17 The double layer capacitances (C_{dl}) of RuO_2-NiO/NF with different RuO_2 loading amount.

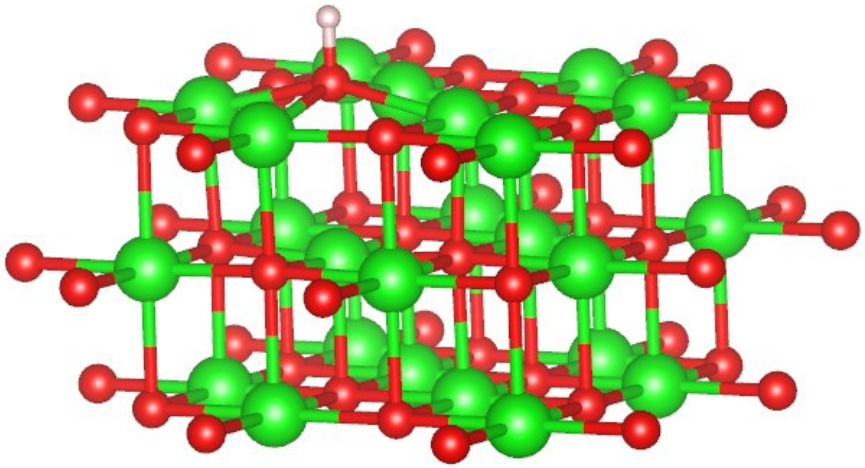

Fig. S18 The optimized geometry of adsorption structure of H on NiO (100).

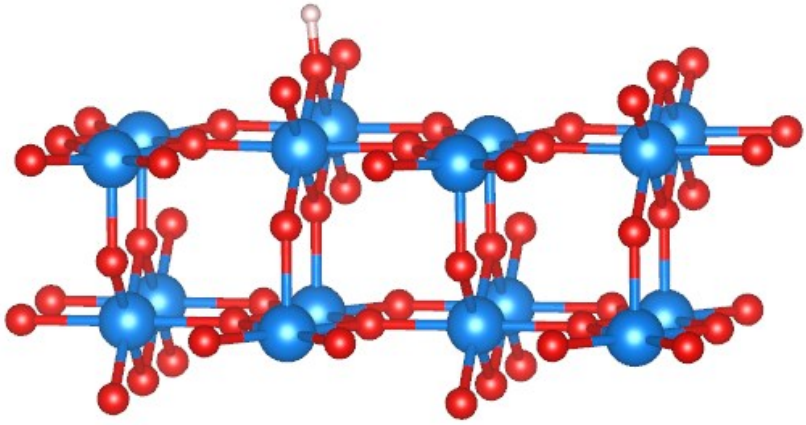

Fig. S19 The optimized geometry of adsorption structure of H on RuO_2 (110).

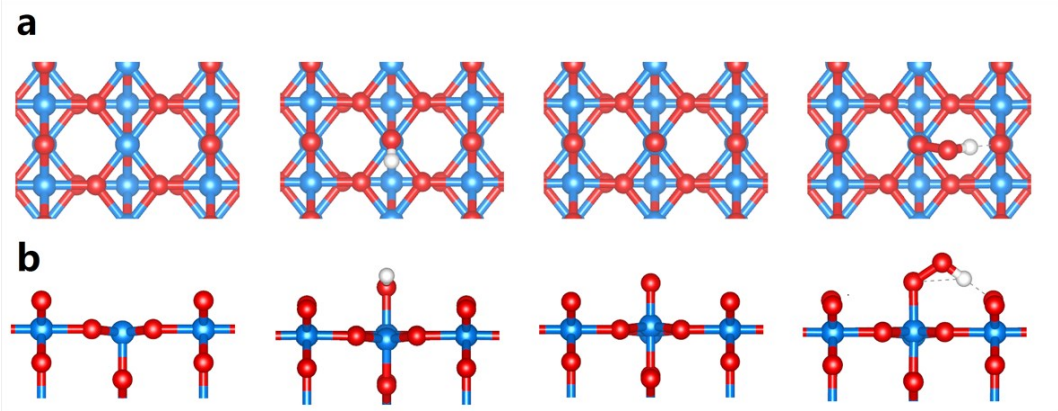

Fig. S20 The (a) top view and (b) side view of the optimized geometry of adsorption structure of OH, O and OOH intermediates on RuO_2 (110).

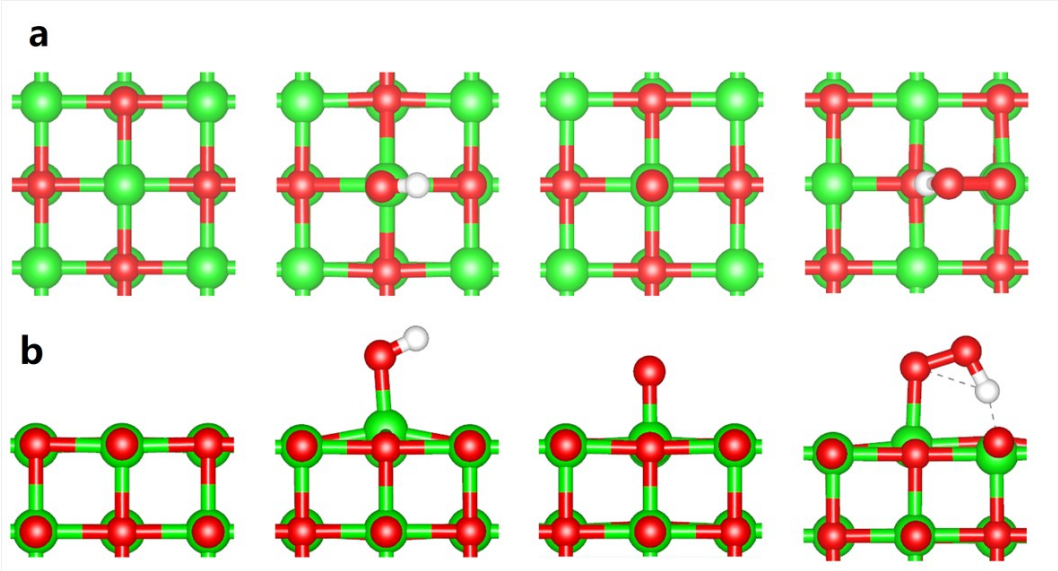

Fig. S21 The (a) top view and (b) side view of the optimized geometry of adsorption structure of OH, O and OOH intermediates on NiO (100).

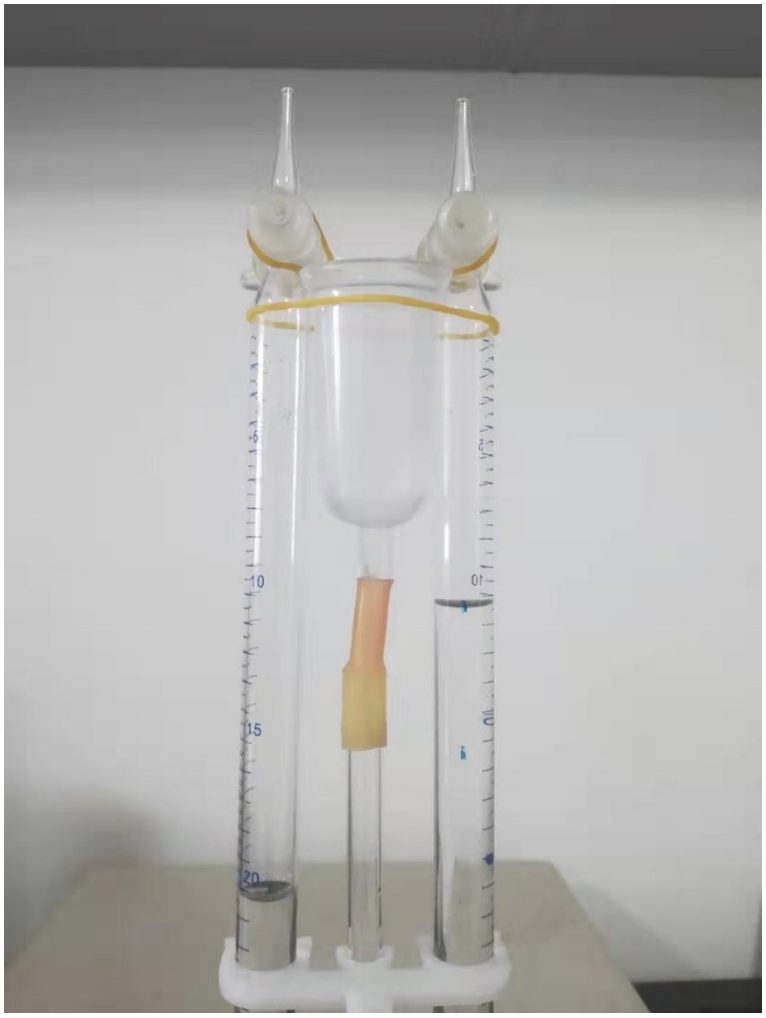

Fig. S22 The optical picture of the measured setup of the Hoffman apparatus.

Table S1. Comparison of the OER performance of RuO_2-NiO/NF with reported catalysts in 1 M KOH. *The value is evaluated from the polarization curves exhibited in literature.

Catalyst	Support	η_{10}, OER(mV)	$J_{1.55}$, OER(mA cm^{-2})	source
RuO_2-NiO	**Nickel foam**	**187**	**482**	**This work**
Ru/Cu-doped RuO_2	Glassy carbon	241	110*	6
RuO_2/N−C	Glassy carbon	280	22*	7
RuO_2/NiO	Nickel foam	250	85*	8
IrO_2@NiO	Nickel foam	278	88*	9
NiO-Cr_2O_3	Glassy carbon	270	15*	10
NiO/CN	Glassy carbon	261	58*	11
CuFe	Nickel foam	218	203*	12
Ni/$Ni(OH)_2$	Carbon paper	270	45*	13
CoP-InNC@CNT	Glassy carbon	270	19*	14
Co-NCNTFs	Nickel foam	230	75*	15
IrRh NAs	Glassy carbon	251	31*	16

Table S2. Comparison of the HER performance of RuO_2-NiO/NF with recently reported catalysts in 1 M KOH. *The value is evaluated from the polarization curves exhibited in literature.

Catalyst	Support	η_{10}, HER(mV)	j_{100}, HER (mA cm^{-2})	source
RuO_2-NiO	**Nickel foam**	**17**	**452**	**This work**
Ru/Cu-doped RuO_2	Glassy carbon	28	72*	6
RuO_2/N−C	Glassy carbon	40	43*	7
Ni@Ni_2P-Ru	Glassy carbon	31	21*	17
$Ni(OH)_2$-$NiMoO_x$	Nickel foam	36	75*	18
Ru@NC	Glassy carbon	27.5	64*	19
NiO NRs	Carbon paper	110	8*	20
Fe-NiO	Nickel foam	88	18*	21
CuFe	Nickel foam	158	4*	12
Ni/$Ni(OH)_2$	Carbon paper	77	28*	13
CoP-InNC@CNT	Glassy carbon	159	3*	14
Co-NCNTFs	Nickel foam	141	7*	15
Ni/NiO	Glassy carbon	90	11*	22

Table S3. Comparison of the overall water splitting performance of RuO_2-NiO/NF with recently reported bifunctional catalysts in 1 M KOH. *The value is evaluated from the polarization curves exhibited in literature.

Catalyst	Support	η_{10}, Overall(V)	$j_{1.7}$, Overall (mA cm^{-2})	source
RuO_2-NiO	**Nickel foam**	**1.43**	**631**	**This work**
Ru/Cu-doped RuO_2	Glassy carbon	1.47	\	6
RuO_2/N−C	Carbon paper	1.534	33*	7
RuO_2/NiO	Nickel foam	1.5	\	8
Fe-NiO	Nickel foam	1.579	\	21
PA-NiO	Nickel foam	1.56	48*	23
CuFe	Nickel foam	1.64	16*	12
Ni/$Ni(OH)_2$	Carbon paper	1.59	60*	13
CoP-InNC@CNT	Carbon cloth	1.58	41*	14
Co-NCNTFs	Nickel foam	1.62	16*	15
hcp-Co@NC	Carbon paper	1.58	16*	24
FeOOH/Ni_3N	Carbon cloth	1.56	48*	25
CoFe-CDs||CoFeRu@C	Glassy carbon	1.59	27*	26
$Ni(S_{0.61}Se_{0.39})_2$@PGCNS	Nickel foam	1.54	113*	27
NiO-GDY NC	Nickel foam	1.52	248*	28
Co-P-S	Nickel foam	1.6	37*	29
$CoFe_2O_4$	Carbon cloth	1.53	57*	30
MoS_2/LDH	Nickel foam	1.57	42*	31
IrRh NAs	Nickel foam	1.57	24*	18
$Co_{0.75}Ni_{0.25}(OH)_2$	Carbon paper	1.56	41*	32
NiVIr LDH	Nickel foam	1.49	137	33
MoS_2/NiS_2	Carbon cloth	1.59	50	34
Ni-Fe NP	Carbon paper	1.47	48*	35

Table S4. Contents of Ru and Ni elements in the electrolyte after the water electrolysis at 1000 mA cm^{-2} as determined by ICP-OES analysis.

Sample	Ru (ng/mL)	Ni (ng/mL)
Post 0-100 h	0.78	5.58
Post 100-200 h	0.58	5.68

References

1 K. Li, Y. Li, Y. Wang, J. Ge, C. Liu, W. Xing, Energ. *Environ. Sci*. 2018, **11**, 1232-1239.

2 Z. J. Chen, G.-X. Cao, L. Y. Gan, H. Dai, N. Xu, M. J. Zang, H. B. Dai, H. Wu, P. Wang, *ACS Catal*. 2018, **8**, 8866-8872.

3 J. Qian, X. Bai, S. Xi, W. Xiao, D. Gao, J. Wang, ACS Appl. *Mater. Inter*. 2019, 11, 30865-30871.

4 Y. Zheng, Y. Jiao, Y. Zhu, L. H. Li, Y. Han, Y. Chen, A. Du, M. Jaroniec, S. Z. Qiao, *Nat. Commun*. 2014, **5**, 1-8.

5 J. Rossmeisl, Z. W. Qu, H. Zhu, G. J. Kroes, J. K. Nørskov, *J. Electroanal. Chem*. 2007, **607**, 83-89.

6 K. Yang, P. Xu, Z. Lin, Y. Yang, P. Jiang, C. Wang, S. Liu, S. Gong, L. Hu, Q. Chen, *Small* 2018, **14**, 1803009.

7 C. Z. Yuan, Y. F. Jiang, Z. W. Zhao, S. J. Zhao, X. Zhou, T. Y. Cheang, A. W. Xu, *ACS Sustain. Chem. Eng*. 2018, **6**, 11529-11535.

8 J. Liu, Y. Zheng, Y. Jiao, Z. Wang, Z. Lu, A. Vasileff, S. Z. Qiao, *Small* 2018, **14**, 1704073.

9 J. Liu, Z. Wang, K. Su, D. Xv, D. Zhao, J. Li, H. Tong, D. Qian, C. Yang, Z. Lu, *ACS Appl. Mater. Inter*. 2019, **11**, 25854-25862.

10 X. Liu, J. Wu, *Electrochim. Acta* 2019, **320**,134577.

11 C. Liao, B. Yang, N. Zhang, M. Liu, G. Chen, X. Jiang, G. Chen, J. Yang, X. Liu, T. S. Chan, *Adv. Funct. Mater*. 2019, **29**, 1904020.

12 A. I. Inamdar, H. S. Chavan, B. Hou, C. H. Lee, S. U. Lee, S. Cha, H. Kim, H. Im, *Small* 2020, **16**, 1905884.

13 L. Dai, Z. N. Chen, L. Li, P. Yin, Z. Liu, H. Zhang, *Adv. Mater*. 2020, **32**, 1906915.

14 L. Chai, Z. Hu, X. Wang, Y. Xu, L. Zhang, T. T. Li, Y. Hu, J. Qian, S. Huang, *Adv. Sci*. 2020, **7**, 1903195.

15 Q. Yuan, Y. Yu, Y. Gong, X. Bi, *ACS Appl. Mater. Inter*. 2020, **12**, 3592-3602.

16 C. Li, Y. Xu, S. Liu, S. Yin, H. Yu, Z. Wang, X. Li, L. Wang, H. Wang, *ACS Sustain. Chem. Eng*. 2019, **7**, 15747-15754.

17 Y. Liu, S. Liu, Y. Wang, Q. Zhang, L. Gu, S. Zhao, D. Xu, Y. Li, J. Bao, Z. Dai, *J. Am. Chem. Soc.* 2018, 140, **8**, 2731-2734.

18 Z. Dong, F. Lin, Y. Yao, L. Jiao, *Adv. Energy Mater.* 2019, **9**, 1902703.

19 Y. Li, L. A. Zhang, Y. Qin, F. Chu, Y. Kong, Y. Tao, Y. Li, Y. Bu, D. Ding, M. Liu, *ACS Catal.* 2018, **8**, 5714-5720.

20 T. Zhang, M. Y. Wu, D. Y. Yan, J. Mao, H. Liu, W. B. Hu, X. W. Du, T. Ling, S. Z. Qiao, *Nano Energy* 2018, **43**, 103-109.

21 Z. Wu, Z. Zou, J. Huang, F. Gao, *J Catal.* 2018, **358**, 243-252.

22 L. Zhao, Y. Zhang, Z. Zhao, Q. Zhang L. Huang, L. Gu, G. Lu, J. Hu, L. Wan, *Natl. Sci. Rev*. 2020, **7**, 27-36.

23 Z. Li, W. Niu, L. Zhou, Y. Yang, *ACS Energy Lett.* 2018, **3**, 892-898.

24 N. Li, H. Tan, X. Ding, H. Duan, W. Hu, G. Li, Q. Ji, Y. Lu, Y. Wang, F. Hu, *Appl. Catal. B: Environ.* 2020, **266**, 118621.

25 J. Guan, C. Li, J. Zhao, Y. Yang, W. Zhou, Y. Wang, G. R. Li, *Appl. Catal. B: Environ.* 2020, **269**, 118600.

26 M. Yang, T. Feng, Y. Chen, J. Liu, X. Zhao, B. Yang, *Appl. Catal. B: Environ.* 2020, **267**, 118657.

27 Y. Zhou, Y. Wang, H. Zhao, J. Su, H. Zhang, Y. Wang, *J. Catal.* 2020, **381**, 84-95.

28 H. Yu, Y. Xue, L. Hui, F. He, C. Zhang, Y. Liu, Y. Fang, C. Xing, Y. Li, H. Liu, *Nano Energy* 2019, **64**, 103928.

29 F. Du, Y. Zhang, H. He, T. Li, G. Wen, Y. Zhou, Z. Zou, *J. Power Sources* 2019, **431**, 182-188.

30 C. Guo, X. Liu, L. Gao, X. Ma, M. Zhao, J. Zhou, X. Kuang, W. Deng, X. Sun, Q. Wei, *J. Mater. Chem. A* 2019, **7**, 21704-21710.

31 P. Xiong, X. Zhang, H. Wan, S. Wang, Y. Zhao, J. Zhang, D. Zhou, W. Gao, R. Ma, T. Sasaki, *Nano lett.* 2019, **19**, 4518-4526.

32 X. Wang, Z. Li, D. Y. Wu, G. R. Shen, C. Zou, Y. Feng, H. Liu, C. K. Dong, X. W. Du, *Small* 2019, **15**, 1804832.

33 S. Li, C. Xi, Y.-Z. Jin, D. Wu, J.-Q. Wang, T. Liu, H.-B. Wang, C.-K. Dong, H. Liu, S. A. Kulinich, *ACS Energy Lett.* 2019, **4**, 1823-1829.

34 J. Lin, P. Wang, H. Wang, C. Li, X. Si, J. Qi, J. Cao, Z. Zhong, W. Fei, J. Feng, *Adv. Sci.* 2019, **6**, 1900246.

35 B. H. Suryanto, Y. Wang, R. K. Hocking, W. Adamson, C. Zhao, *Nat. Commun.* 2019, **10**, 1-10.